Published in final edited form as:
Int J Radiat Oncol Biol Phys. 2014 February 1; 88(2): 404–411. doi:10.1016/j.ijrobp.2013.10.037.

A non-human primate model of human radiation-induced venocclusive liver disease and hepatocyte injury

Govardhana Rao Yannam[#1], **Bing Han**[#2,3], **Kentaro Setoyama**[#2], **Toshiyuki Yamamoto**[1], **Ryotaro Ito**[2], **Jenna M. Brooks**[2], **Jorge Guzman-Lepe**[2,4], **Csaba Galambos**[4], **Jason V. Fong**[2], **Melvin Deutsch**[5], **Mubina A. Quader**[5], **Kosho Yamanouchi**[6,7], **Rafi Kabarriti**[6], **Keyur Mehta**[6], **Alejandro Soto-Gutierrez**[4,8], **Jayanta Roy-Chowdhury**[7,9], **Joseph Locker**[7,10], **Michio Abe**[11], **Charles A. Enke**[11], **Janina Baranowska-Kortylewicz**[11], **Timothy D. Solberg**[12], **Chandan Guha**[6,7,10], and **Ira J. Fox**[2,8]

[1]Department of Surgery, University of Nebraska Medical Center, Omaha, NE, United States

[2]Department of Surgery, University of Pittsburgh, Pittsburgh, PA, United States

[3]Department of Hepatobiliary Surgery, First Affiliated Hospital of Xi'an Jiaotong University, Xi'an, Shaanxi, China

[4]Department of Pathology, Children's Hospital of Pittsburgh, Pittsburgh, PA, United States

[5]Department of Radiation Oncology, Children's Hospital of Pittsburgh, Pittsburgh, PA, United States

[6]Department of Radiation Oncology, Albert Einstein College of Medicine, Bronx, NY, United States

[7]Marion Bessin Liver Research Center, Albert Einstein College of Medicine, Bronx, NY, United States

[8]McGowan Institute for Regenerative Medicine, University of Pittsburgh, Pittsburgh, PA, United States

[9]Department of Medicine (Hepatology Division), Albert Einstein College of Medicine, Bronx, NY, United States

[10]Department of Pathology, Albert Einstein College of Medicine, Bronx, NY, United States

[11]Department of Radiation Oncology, University of Nebraska Medical Center, Omaha, NE, United States

[12]Department of Radiation Oncology, University of Texas Southwestern, Dallas, TX, United States

[#] These authors contributed equally to this work.

All communications should be addressed to Ira J, Fox, Department of Surgery, Children's Hospital of Pittsburgh of UPMC, Children's Hospital Drive, 45th and Penn, Pittsburgh PA 15201, Tel. (412) 692-6671, Fax (412) 692-6599, foxi@upmc.edu or Chandan Guha, Departments of Radiation Oncology and Pathology, Marion Bessin Liver Research Center, Albert Einstein College of Medicine, Ullman Bldg, Bronx, NY 10461, Tel (718) 430-3556; cguha@montefiore.org.

Conflict of interest: The authors report no conflict of interest

Abstract

Background—Human liver has an unusual sensitivity to radiation that limits its use in cancer therapy or in preconditioning for hepatocyte transplantation. Since the characteristic venocclusive lesions of radiation-induced liver disease do not occur in rodents, there has been no experimental model to investigate the limits of safe radiation therapy or explore the pathogenesis of hepatic venocclusive disease.

Methods—We performed a dose escalation study in a primate, the cynomolgus monkey, using hypofractionated stereotactic body radiotherapy in 13 animals.

Results—At doses ≥40Gy, animals developed a systemic syndrome resembling human radiation-induced liver disease, consisting of decreased albumin, elevated alkaline phosphatase, loss of appetite, ascites, and normal bilirubin. Higher radiation doses were lethal, causing severe disease that required euthanasia approximately 10 weeks after radiation. Even at lower doses where radiation-induced liver disease was mild or non-existent, latent and significant injury to hepatocytes was demonstrated by asialoglycoprotein-mediated functional imaging. These monkeys developed hepatic failure with encephalopathy when they received parenteral nutrition containing high concentrations of glucose. Histologically, livers showed central obstruction via an unusual intimal swelling that progressed to central fibrosis.

Conclusions—The cynomolgus monkey, as the first animal model of human venocclusive radiation-induced liver disease, provides a resource for characterizing the early changes and pathogenesis of venocclusion, for establishing nonlethal therapeutic dosages, and for examining experimental therapies to minimize radiation injury.

Keywords

hepatic irradiation; radiation induced liver disease; acute liver failure; non-human primates; asialoglycoprotein receptor-based nuclear scan

INTRODUCTION

Radiation therapy (RT) has great utility for treatment of cancer and host conditioning for bone marrow transplantation. More recently, preparative irradiation has facilitated the transplantation of hepatocytes, neural, and mesenchymal cells [20,21,32]. However, this utility is limited by significant morbidity, even mortality, associated with hepatic irradiation. Clinically, whole liver irradiation has been restricted to 30–35 Gy in standard daily fractions of 1.8–2 Gy, as patients may develop lethal radiation induced liver disease (RILD) above these dose levels. Recent technological advances, such as, intensity modulated RT (IMRT), three-dimensional conformal RT (3DCRT) planning, and organ and tumor motion tracking — have enabled treatment of liver cancer with fewer (1–6) but larger dose fractions (5–24 Gy), a procedure termed hypofractionated stereotactic body RT (SBRT). Although several trials have demonstrated the safety and effectiveness of SBRT [24,31], RILD still limits its clinical application.

Patients with RILD usually present with fatigue, weight gain, hepatomegaly, ascites, and an isolated elevation in alkaline phosphatase (ALP) within four months of hepatic RT [18]. The characteristic initial finding of normal serum bilirubin and ammonia levels indicates that classic RILD does not cause liver failure. Instead, the histopathological appearance of RILD in humans is one of venocclusive disease (VOD), predominantly of the central and sublobular hepatic veins, with sparing of the arteries and periportal vessels [7,26,28]. Although various forms of RILD occur in animals, whole-liver irradiation failed to produce VOD in rats [11,13], dogs [8] and rhesus monkeys [29].

We studied cynomolgus monkeys to determine whether hypofractionated liver RT would generate VOD similar to irradiated human liver and in contrast to rodent radiation responses.

METHODS

Animals and Radiation treatment

Anesthetized, male cynomolgus monkeys (5–9 kg) received initial doses of 30, 36, 40, and 50 Gy in five consecutive daily fractions, using 6 MV energy photon beams from an ONCOR linear accelerator (Siemens Oncology Systems, Erlangen, Germany), according to plans to whole liver (supplementary information). Since the monkeys receiving 30–36 Gy to whole liver developed minimal clinical symptoms, they received additional fractions to partial liver segments (36 Gy single course, 50 Gy single course, 7.2 Gy × 3 consecutive daily fractions followed by 8 Gy × 2 consecutive daily fractions n=2) totaling up to 85.6 Gy, 6–12 months after original liver irradiation.

Assessment of radiation effect by ASGPR-based SPECT imaging

Asialofetuin (AF)-(^{99m}Tc-SHNH)$_6$ with a specific activity of about 90 μCi^{99m}Tc/μg (3.33 MBq/μg) was synthesized as described [1,25]. A single 2 mCi (74 MBq) bolus dose of ^{99m}Tc(SHNH)$_6$-AF was injected into the central venous catheter line of anesthetized monkeys. Prior to imaging, a 100-mL saline bag containing 1 mCi ^{99m}Tc was scanned as a calibration standard, using data acquisition parameters from the animal imaging protocol. Counts at 30 sec, 1 min, and 2 min, and the average activity/pixel/min were calculated. Subsequent scans were normalized to the total counts in the “calibration” scan, enabling quantitative comparison among animals. The times of calibration imaging, injection, and planar and SPECT imaging studies were carefully monitored to correlate scan data with activity.

TPN

Monkeys (n=4) were given TPN, 1–9 months after the radiation treatment because of weight loss. TPN solution (without lipids)—10%–25% Dextrose, 1.8% amino acid, electrolytes (sodium and potassium), trace elements, carnitine, and insulin—was infused continuously at a maintenance level of 70 ml/kg/day through a central venous catheter.

Histology and Immunohistochemistry

Liver specimens were fixed in 4% paraformaldehyde, and 4-μm sections were prepared from paraffin-embedded specimens. Histological analysis utilized hematoxylin and eosin, reticulin, and Masson's trichrome staining. To assess macrophage infiltration, immunohistochemistry was performed using a mouse monoclonal antibody to CD163 (1:250, Vector Laboratories), CC1 antigen retrieval (Ventana Medical Systems), DAB detection, and a hematoxylin counterstain.

RESULTS

Biologic effects of whole liver hypofractionated radiation therapy

To establish the whole liver tolerance to irradiation, a dose escalation (30, 36, 40, and 50 Gy) study was performed using hypofractionated radiation therapy in 5 consecutive daily fractions. Animals were monitored for one to two years for toxicity by weekly blood test, body weight, and objective scoring of activity and appetite level. Additional studies included histologic analysis of biopsies and functional assessment via ASGPR-mediated molecular imaging.

Animals treated with 30–36 Gy (n=7) developed no serious hepatic or systemic consequences from hypofractionated radiation therapy. ALT increased to 140–250 IU/L, 5–10 weeks after completion of hypofractionated radiation therapy. ALP followed a similar pattern (Fig. 1). However, albumin levels fell dramatically and required more than 6 months to return to normal. Bilirubin levels remained normal and there was no development of ascites.

No animals receiving 40 Gy (n=3) developed liver failure. Two animals developed gastrointestinal ulcers secondary to collateral radiation injury, 8 and 9 weeks after completion of RT, presumed to be from excursion into the treatment field during respiration. Approximately 10 weeks following radiation, the remaining animal developed a systemic syndrome resembling human RILD, with decreased albumin, increased ALP, and severe loss of appetite and weight. The animal remained ill for more than 22 weeks, and while the course stabilized, the animal did not return to normal behavior or weight. While no animal receiving 50 Gy (n=3) developed liver failure, they developed a more severe form of RILD approximately 10 weeks following radiation with 100% mortality. This process was associated with the above findings, but also vomiting and development of ascites. In all animals, bilirubin, prothrombin time, and ammonia levels were normal, and there was no evidence of hepatic encephalopathy.

Histologically, the livers showed injury to hepatic central veins, most severe in small venules, with significant extension to larger central veins at higher radiation dosage. At 30–36 Gy, central veins showed only mild medial fibrosis, and occasional prominent endothelial cells, but not intimal swelling. There were a few subendothelial inflammatory cells but the lumens were not narrowed or occluded (Fig. 2A, B). Early after the intermediate dose of 40 Gy, central veins showed moderate subendothelial edema and hemorrhage in the intima. There was also moderate fibrosis that extended into the adjacent sinusoid with mild congestion (Fig. 2E,F). Animals that received ≥40 Gy had marked venocclusive changes in the central veins. The pathology in these vessels was primarily within the intima, which was edematous and hemorrhagic. These changes raised the endothelium and narrowed or completely obstructed the lumen. The media showed mild fibrosis, with areas of sinusoidal congestion and fibrosis (Fig. 2D, E). The changes were most severe in animals that developed RILD after receiving liver re-irradiation.

In all animals treated with liver-directed hypofractionated radiation therapy there was a significant time-dependent reduction in hepatocyte receptor function as determined by ASGPR-mediated imaging studies (Fig. 3A, B). The alteration in modified ASGPR index persisted for more than a year after RT, and was associated with a corresponding rise in ASGPR ligand clearance indices, apparently reflecting impaired expression of this receptor. Hepatic ASGPR function decreased to 40–60% of pre-treatment values after a single course of radiation therapy.

Finally, in light of the potential clinical application of focal hepatic irradiation, we also examined the consequences of delivering RT to less than the whole liver in one monkey. Six months after receiving 36 Gy to the right lobe of the liver (Fig. 3C), ASGPR-mediated SPECT imaging detected mild atrophy of the irradiated section of the liver and compensatory hypertrophy of the un-irradiated left lobe of the liver that maintained normal hepatic function and ASGPR activity.

Biologic effects of re-irradiation after hepatic hypofractionated radiation therapy

We next examined the consequences of re-irradiation of liver by hypofractionated radiation therapy (N=4). All monkeys initially received 30–36 Gy, which resulted in only minimal clinical symptoms and minor histopathologic changes in the liver. Thereafter, animals

received one or two additional sessions of hypofractionated radiation therapy at six month to 1 year intervals.

Two animals that received 36 and or 50 Gy of additional partial liver hypofractionated radiation therapy were euthanized with RILD (14 weeks after 36 Gy and 9 weeks after 50 Gy, respectively). Light microscopy showed central venous luminal obstruction from subendothelial edema and hemorrhage, with central sinusoidal congestion (Fig. 2D, E). Some livers also showed areas of portal-portal bridging fibrosis, but this change was irregular (not illustrated).

A lower second dose of liver-directed hypofractionated radiation therapy did not produce RILD (n=2, 7.2 Gy × 3), although ASGPR-based imaging and receptor uptake/ clearance ratios demonstrated progressive alteration in the shape and function of the liver (Fig. 3 and e1). Subsequent dosing of these two animals with 16 Gy (8 Gy × 2), six months after the second treatment, increased portal-portal fibrosis but did not induce RILD or chronic liver failure.

Sensitivity of the irradiated liver to stress: induction of fulminant hepatic failure

After whole liver hypofractionated radiation therapy, animals lost body weight despite adequate feeding. We therefore, administered TPN to provide additional nutritional support in these animals, starting with low dextrose load (10%) to avoid hyperglycemia, then increased after 1–2 weeks. Unexpectedly, these animals developed acute liver failure. Four monkeys received TPN following high dose liver-directed radiation therapy (≥36 Gy). TPN with 10% dextrose did not produce changes in liver function tests or enzymes. But, when TPN contained 15–20% dextrose, liver function tests became abnormal. Within one week ALP levels increased up to 15x control; serum albumin decreased to 2.0–2.2 g/dl (control 3–3.5 g/dl); and plasma ammonia increased up to twice control. Bilirubin and prothrombin time, however, did not change. Liver function tests remained at this level until the concentration of dextrose in the TPN was increased up to 25%. At this point all animals developed hepatic failure and required euthanasia. Within one week of TPN with 25% dextrose, ALP increased up to 60x control, plasma ammonia increased up to 5x control, and serum bilirubin increased to 7–30x control. In addition, prothrombin times prolonged to 16.5–32 sec (control 14.0 sec) and all monkeys became severely encephalopathic. Their irreversible liver failure necessitated euthanization approximately 10 days after instituting TPN with high concentration dextrose.

Liver histology demonstrated irregular regions of coagulative hepatic necrosis, hepatocyte dropout, and microvesicular steatosis, with fibrin deposition, hemorrhage, and focal clusters of hemosiderin-laden macrophages. The necrotic process involved both portal and central areas (Fig. 4). In places, the disappearing liver cells left loose connective tissue behind that was infiltrated by macrophages and a few lymphoid cells. Reticulin network condensation and fragmentation was evident at the sites of necrosis. No significant arterial damage was seen, and no cholestasis, although there was epithelial injury in smaller bile ducts. At higher magnification, central and portal vein endothelial injury with subintimal edema and scattered inflammatory cells caused luminal narrowing. Further documenting the presence of hepatic encephalopathy, post-mortem examination of brain tissue from one animal showed characteristic Alzheimer type II astrocytes with chromatin displacement (Fig. 4F).

DISCUSSION

Classic human RILD and its associated vascular changes have been difficult to reproduce in animal models [1–3]. Our use of cynomolgus monkeys and large fraction sizes of hypofractionated radiation therapy may have been responsible for our ability to produce

radiation-induced hepatic VOD in these studies. We also demonstrated that radiation induced a subtle form of non-classic, atypical RILD, which is related to hepatocyte injury. This correlated with changes in ASGPR activity, which was documented using SPECT imaging of ^{99m}Tc-labeled asialofetuin. The ASGPR scan allowed monitoring of regional variations in hepatic function of irradiated livers. The hepatic insults that occurred following whole liver irradiation, which did not lead to classic RILD, were later uncovered when TPN produced substantial injury to the irradiated hepatocytes and generated hepatic failure.

This is the first report of whole liver radiation tolerance in nonhuman primates after hypofractionated radiation therapy. The monkey liver appears to reproduce the vascular sensitivity to irradiation characteristic of human liver, as lethal RILD was induced after exposure to irradiation doses over 40 Gy. This is an interesting finding because despite differences in sensitivity to pathological radiation injury across species, hepatic venous injury was radiation dose-dependent in cynomolgus monkeys. The pathological hallmark of RILD, venocclusive lesions, has been previously described as complete obliteration of central vein lumina by erythrocytes trapped in a dense network of reticulin and collagen fibers that crisscross the lumen of the central veins, sublobular veins, and centrilobular sinusoids [9]. In patients that do not succumb to RILD, vascular congestion resolves after several months as the liver gradually begins to heal. The hepatic architecture, however, remains distorted, with persistent fibrosis of central veins and unrepaired centrilobular collapse throughout the affected region [18]. Human studies have stressed the thrombotic component of central venous injury following liver irradiation [9,27]. In our studies of cynomolgus monkeys, however, thrombosis was only a minor part of the obliterative process. The radiation-induced endothelial injury resulted in a sinusoidal obstruction syndrome (SOS), which was similar to the hepatic injury induced by administration of monocrotaline in *Macaca speciosa* monkeys [2], and to human SOS induced by chemotherapy, with or without RT, in patients undergoing allogeneic bone marrow transplantation [7]. Among other lesions, human SOS shows edematous widening of the subendothelial space of central and sublobular veins [26,28]. Our studies of the monkey liver following hypofractionated radiation therapy suggest that this edema, and subsequent hemorrhage into the enlarged subendothelial space, is the main cause of outflow obstruction. Sinusoidal congestion and hepatocyte damage are likely secondary to this obstruction. The change apparently results from a distinctive radiation sensitivity of human and monkey central vein endothelium that is not reproduced in irradiated rodents.

As in classic RILD of humans [12,18], liver failure and hepatic encephalopathy were not seen in monkeys. Previously healthy monkeys developed disinterest in food, diminished activity, low serum albumin, and ascites after very high doses of liver irradiation, but without liver failure or encephalopathy. Many of these findings could be secondary to an acute phase response produced by radiation-induced release of cytokines, such as, IL-1, IL-6 and TNFα [6,17,22].

Radiation-induced hepatocellular injury as a component of RILD is underappreciated. It is generally believed to be a secondary phenomenon resulting from atrophy of perivenous hepatocytes due to inadequate blood supply and hypoxia. Our studies indicate that radiation produces a degree of hepatocellular injury that is not appreciated in functionally stable, irradiated livers, which may have normal metabolic function. The injury is revealed, however, by relatively minor insults such as administration of TPN. Chronic TPN use has been shown in humans and animal models to lead to hepatic dysfunction by different mechanisms including oxidative injury and apoptosis of hepatocytes [4, 5]. Even 1 week of TPN containing 15–20% dextrose use which would typically induce steatosis alone, caused substantial hepatic necrosis and acute liver failure in monkeys that received liver irradiation. Loss of hepatocellular regeneration capacity is another consequence of hepatic irradiation

[10,13] and may render the irradiated liver incapable of the compensation that prevents irreversible hepatic failure.

CT-based imaging studies have demonstrated deformation and atrophy of the irradiated liver and expansion of un-irradiated segments of the liver [16,33], but they have not been used previously for measuring anatomic changes in hepatic function resulting from RT. Dynamic contrast-enhanced CT and indocyanine green (ICG) clearance studies have been performed following conformal RT of the liver in cancer patients [4,5] and showed that hepatic perfusion is reduced and ICG clearance is delayed following liver RT. However, ICG clearance is unable to identify regional variations in hepatic function. Our studies used ASGPR molecular imaging with SPECT to monitor regional variations in hepatic function. ASGP receptors are found in abundance on the sinusoidal surface of hepatocytes, and initial ^{99m}Tc-labeled asialofetuin uptake is determined by hepatic blood flow. However, after equilibration, receptor concentration and receptor-mediated endocytosis by hepatocytes become the determining factors. SPECT imaging was used to identify volume and anatomic data indicating functioning and non-functioning portions of the liver [14,15]. Our results demonstrated a radiation dose-dependent reduction in ASGPR-mediated uptake of radiolabeled ligands. Significantly, diminished uptake was seen in atrophic liver segments, while enlarged nonirradiated liver segments showed increased uptake. This segmental variation supports the concept that the liver would tolerate regionally focused high-dose radiation treatment. More importantly, ASGPR-based imaging could potentially be used to assess the hepatocyte-specific effects of radiation therapy, as the loss of receptor activity correlated with the later risk of hepatic dysfunction uncovered following minimal insults to the liver.

Despite the availability of numerous surgical and pharmacologic-based animal models of acute hepatic failure, none recapitulate clinical hepatic failure to the point where the efficacy of cell transplantation or liver assist devices could be predicted in patients. To be effective for assessing the efficacy of therapies, liver failure must be the unequivocal cause of death, and the time to death from liver failure must allow therapy to be introduced after failure has been established, as would be the case clinically [23]. Since clinical experience with auxiliary orthotopic liver transplant for acute hepatic failure [30] indicates that native liver recovery may take 6 months to a year, relevant liver recovery in an animal model would also require an extended time interval. This paper describes a model of acute hepatic failure that meets the above requirements and moreover utilizes a non-human primate that is physiologically similar to man. The model therefore has unique utility for evaluation of human therapies in the treatment of acute liver failure.

In summary, we have shown that non-human primates develop dose-dependent responses to liver-directed hypofractionated radiation therapy similar to those found in man and, at high doses of radiation, develop characteristics of classic human RILD. The critical event appears to be a distinctive radiation injury to central vein endothelium found in humans and higher primates but not rodents. In addition, following intermediate doses of whole liver irradiation that do not lead to lethal RILD, relatively mild hepatic insults significantly injure the irradiated hepatocytes resulting in acute liver failure, and this radiation-induced hepatocyte-specific injury can be assessed anatomically by imaging for asialoglycoprotein receptor activity.

Supplementary Material

Refer to Web version on PubMed Central for supplementary material.

Acknowledgments

This work was supported by the NIH grants: RO1s DK46057, DK67440, and DK68216 (to JRC); DOD PC102137 (to TDS); R01 DK64670 and R21/R33 CA121051 (to CG); and RO1s AI49472, and DK48794 (to IJF).

Abbreviations

3DCRT	3-dimensional Conformal Radiation Therapy
ALP	Alkaline phosphatase
ALT	alanine aminotransferase
ASGPR	asialoglycoprotein receptor
CT	Computerized Tomography
CTV	Clinical Target Volume
GI	Gastrointestinal
IMRT	intensity modulated RT
PTV	Planning Target Volume
RILD	radiation induced liver disease
RT	radiation therapy
SBRT	stereotactic body RT
SOS	sinusoidal obstruction syndrome
SPECT	single-photon emission computerized tomography
TPN	total parenteral nutrition
VOD	venocclusive disease

REFERENCES

[1]. Abe M, Lai J, Kortylewicz ZP, et al. Radiolabeled constructs for evaluation of the asialoglycoprotein receptor status and hepatic functional reserves. Bioconjugate chemistry. 2003; 14:997–1006. [PubMed: 13129404]

[2]. Allen JR, Carstens LA, Olson BE. Veno-occlusive disease in macaca speciosa monkeys. Am J Pathol. 1967; 50:653–667. [PubMed: 4960562]

[3]. Cai W, Wu J, Hong L, et al. Oxidative injury and hepatocyte apoptosis in total parenteral nutrition-associated liver dysfunction. Journal of pediatric surgery. 2006; 41:1663–1668. [PubMed: 17011265]

[4]. Cao Y, Pan C, Balter JM, et al. Liver function after irradiation based on computed tomographic portal vein perfusion imaging. Int J Radiat Oncol Biol Phys. 2008; 70:154–160. [PubMed: 17855011]

[5]. Cao Y, Platt JF, Francis IR, et al. The prediction of radiation-induced liver dysfunction using a local dose and regional venous perfusion model. Med Phys. 2007; 34:604–612. [PubMed: 17388178]

[6]. Cengiz M, Akbulut S, Atahan IL, et al. Acute phase response during radiotherapy. Int J Radiat Oncol Biol Phys. 2001; 49:1093–1096. [PubMed: 11240251]

[7]. DeLeve LD, Shulman HM, McDonald GB. Toxic injury to hepatic sinusoids: Sinusoidal obstruction syndrome (veno-occlusive disease). Semin Liver Dis. 2002; 22:27–42. [PubMed: 11928077]

[8]. Epstein RB, Min KW, Anderson SL, et al. A canine model for hepatic venoocclusive disease. Transplantation. 1992; 54:12–16. [PubMed: 1631920]

[9]. Fajardo LF, Colby TV. Pathogenesis of veno-occlusive liver disease after radiation. Arch Pathol Lab Med. 1980; 104:584–588. [PubMed: 6893535]

[10]. Geraci JP, Mariano MS. Radiation hepatology of the rat: The effects of the proliferation stimulus induced by subtotal hepatectomy. Radiat Res. 1994; 140:249–256. [PubMed: 7938474]

[11]. Geraci JP, Mariano MS, Jackson KL. Hepatic radiation injury in the rat. Radiat. Res. 1991; 125:65–72. [PubMed: 1824725]

[12]. XXXXXXXXXXXXXXXXXX

[13]. XXXXXXXXXXXXXXXXXX

[14]. Hoefs JC, Chen PT, Lizotte P. Noninvasive evaluation of liver disease severity. Clinics in liver disease. 2006; 10:535–562. viii–ix. [PubMed: 17162227]

[15]. Iguchi T, Sato S, Kouno Y, et al. Comparison of tc-99m-gsa scintigraphy with hepatic fibrosis and regeneration in patients with hepatectomy. Annals of nuclear medicine. 2003; 17:227–233. [PubMed: 12846545]

[16]. Jeffrey RB Jr. Moss AA, Quivey JM, et al. Ct of radiation-induced hepatic injury. AJR. American journal of roentgenology. 1980; 135:445–448. [PubMed: 6773363]

[17]. Koc M, Taysi S, Sezen O, et al. Levels of some acute-phase proteins in the serum of patients with cancer during radiotherapy. Biological & pharmaceutical bulletin. 2003; 26:1494–1497. [PubMed: 14519962]

[18]. Lawrence TS, Robertson JM, Anscher MS, et al. Hepatic toxicity resulting from cancer treatment. International Journal of Radiation Oncology, Biology, Physics. 1995; 31:1237–1248.

[19]. Loff S, Kranzlin B, Moghadam M, et al. Parenteral nutrition-induced hepatobiliary dysfunction in infants and prepubertal rabbits. Pediatric surgery international. 1999; 15:479–482. [PubMed: 10525903]

[20]. Marshall GP 2nd, Scott EW, Zheng T, et al. Ionizing radiation enhances the engraftment of transplanted in vitro-derived multipotent astrocytic stem cells. Stem Cells. 2005; 23:1276–1285. [PubMed: 16051984]

[21]. Mouiseddine M, Francois S, Semont A, et al. Human mesenchymal stem cells home specifically to radiation-injured tissues in a non-obese diabetes/severe combined immunodeficiency mouse model. The British journal of radiology. 2007; 80(Spec No 1):S49–55. [PubMed: 17704326]

[22]. Mouthon MA, Vandamme M, van der Meeren A, et al. Inflammatory response to abdominal irradiation stimulates hemopoiesis. International journal of radiation biology. 2001; 77:95–103. [PubMed: 11213354]

[23]. Newsome PN, Plevris JN, Nelson LJ, et al. Animal models of fulminant hepatic failure: A critical evaluation. Liver Transpl. 2000; 6:21–31. [PubMed: 10648574]

[24]. Rusthoven KE, Kavanagh BD, Cardenes H, et al. Multi-institutional phase i/ii trial of stereotactic body radiation therapy for liver metastases. Journal of clinical oncology : official journal of the American Society of Clinical Oncology. 2009; 27:1572–1578. [PubMed: 19255321]

[25]. Schwartz AL. Trafficking of asialoglycoproteins and the asialoglycoprotein receptor. Targeted diagnosis and therapy. 1991; 4:3–39. [PubMed: 1797161]

[26]. Shulman HM, Fisher LB, Schoch HG, et al. Veno-occlusive disease of the liver after marrow transplantation: Histological correlates of clinical signs and symptoms. Hepatology. 1994; 19:1171–1181. [PubMed: 8175139]

[27]. Shulman HM, Gown AM, Nugent DJ. Hepatic veno-occlusive disease after bone marrow transplantation. Immunohistochemical identification of the material within occluded central venules. Am J Pathol. 1987; 127:549–558. [PubMed: 2438942]

[28]. Shulman HM, McDonald GB, Matthews D, et al. An analysis of hepatic venocclusive disease and centrilobular hepatic degeneration following bone marrow transplantation. Gastroenterology. 1980; 79:1178–1191. [PubMed: 7002704]

[29]. Stephens LC, Peters LJ, Ang KK. Tolerance of rhesus monkey liver to ionizing radiation. Radiation Oncology Investigations. 1994; 1:279–284.

[30]. Sudan DL, Shaw BW Jr. Fox IJ, et al. Long-term follow-up of auxiliary orthotopic liver transplantation for the treatment of fulminant hepatic failure. Surgery. 1997; 122:771–777. discussion 777–778. [PubMed: 9347855]

[31]. Tse RV, Hawkins M, Lockwood G, et al. Phase i study of individualized stereotactic body radiotherapy for hepatocellular carcinoma and intrahepatic cholangiocarcinoma. Journal of clinical oncology : official journal of the American Society of Clinical Oncology. 2008; 26:657–664. [PubMed: 18172187]

[32]. Yamanouchi K, Zhou H, Roy-Chowdhury N, et al. Hepatic irradiation augments engraftment of donor cells following hepatocyte transplantation. Hepatology. 2008; 49:258–267. [PubMed: 19003915]

[33]. Yamasaki SA, Marn CS, Francis IR, et al. High-dose localized radiation therapy for treatment of hepatic malignant tumors: Ct findings and their relation to radiation hepatitis. AJR. American journal of roentgenology. 1995; 165:79–84. [PubMed: 7785638]

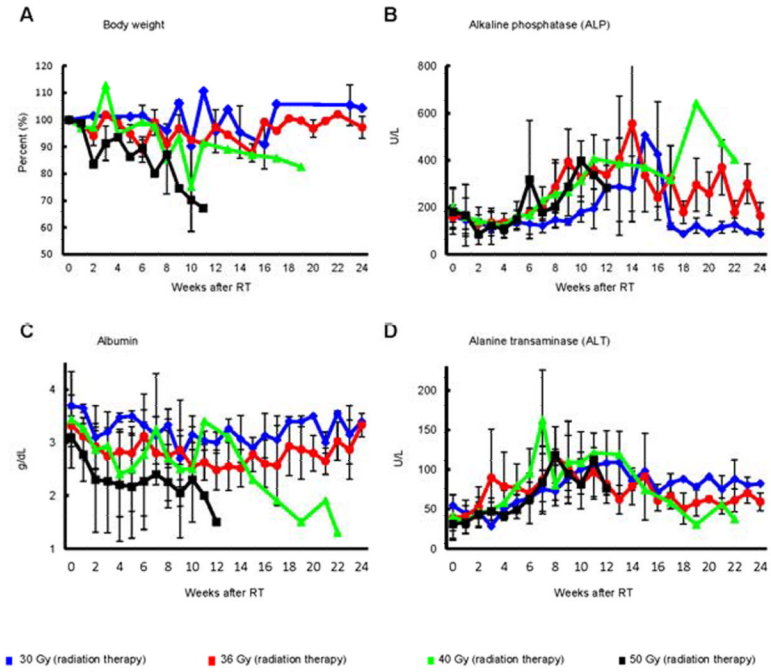

Fig. 1. Body weight and blood parameters in Cynomolgus monkeys that received whole liver hypofractionated radiation therapy (30–50 Gy)

(A) body weight, (B) ALP, (C) albumin and (D) ALT.

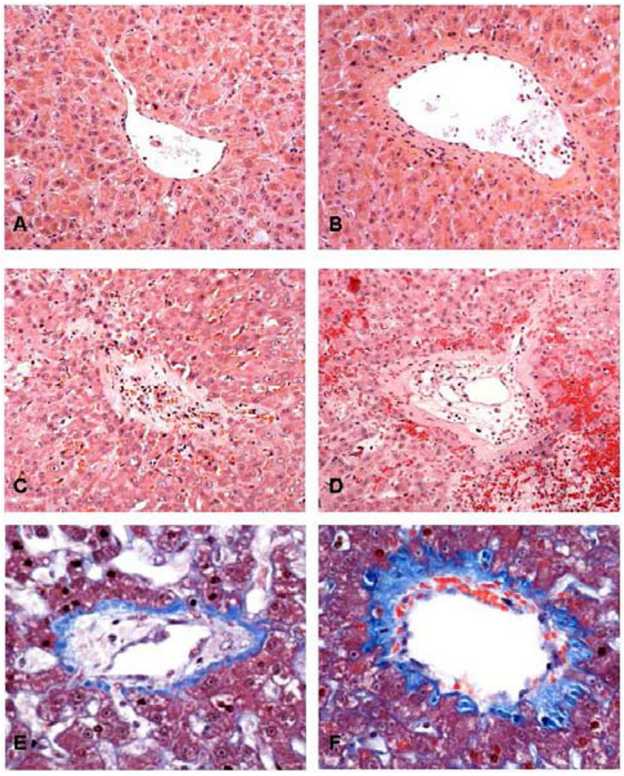

Fig. 2. Hepatic outflow tract histopathology following liver hypofractionated radiation therapy

Hepatic venules (A, C, E) and central veins (B, D, F). (A, B) 30 Gy made endothelium prominent but without luminal compromise. Treatments totaling 66 Gy (C,D) obliterated the venule (C) with recanalization by small vascular channels. (D) Intimal expansion of the central vein by edema and extravasated red cells reduced the lumen to small endothelium-lined channels. Surrounding liver shows congestion, sinusoidal fibrosis, and hepatocyte atrophy. Changes were intermediate after 40 Gy (E, F), with moderate fibrosis extending to surrounding sinusoids. A–D, Hematoxylin and eosin, 20X. E, F,Trichrome, 40X.

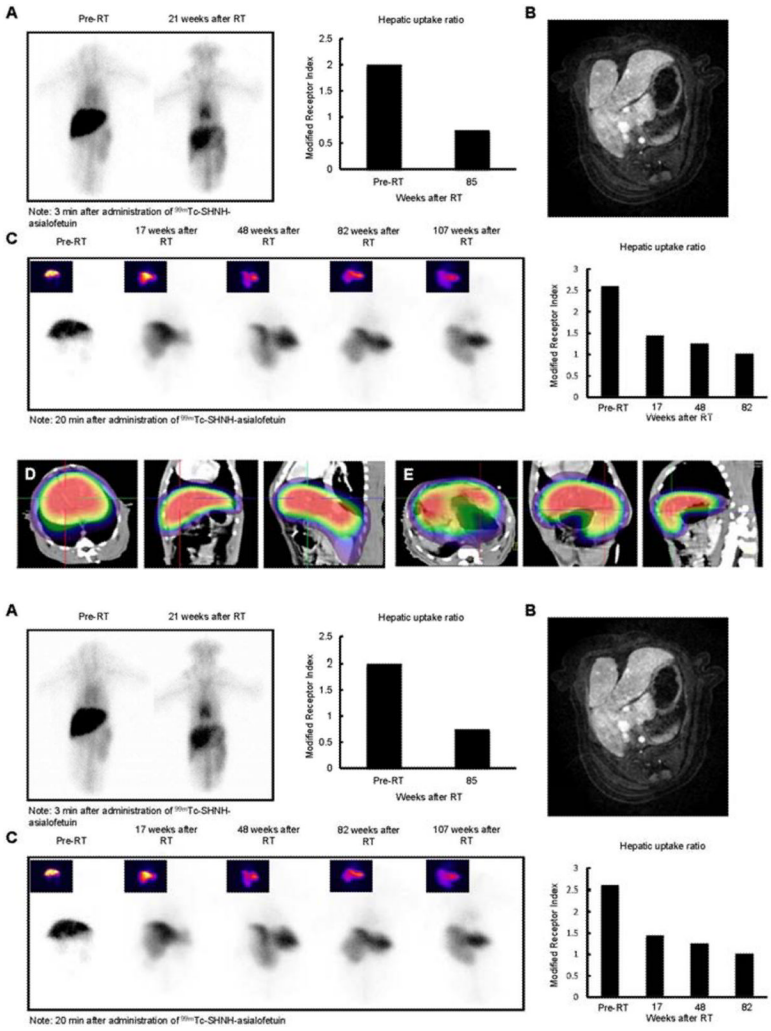

Fig. 3. SPECT-CT images after hepatic irradiation

(A) ASGPR planar dynamic scans and modified receptor indices (hepatic uptake ratios) pre- and 21-weeks post 30 Gy whole liver RT. (B) Two years after completion of 36 Gy partial liver hypofractionated radiation therapy, an MR scan shows marked enlargement of the nonirradiated liver. (C) Planar ASGPR-based nuclear imaging shows altered morphology and progressive worsened ASGPR function in the irradiated liver lobe. Changes were quantified by the modified receptor index.

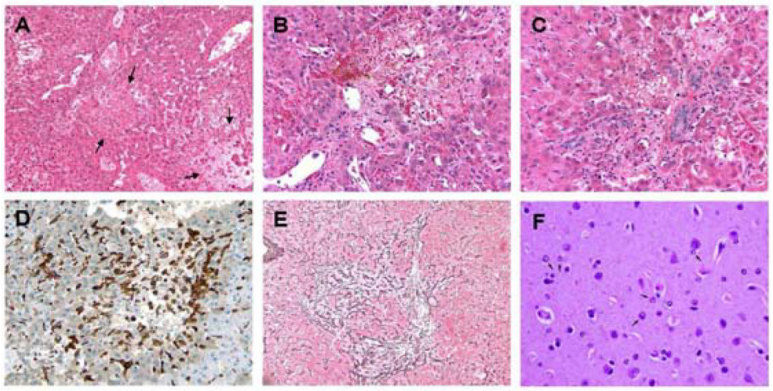

Fig. 4. Histopathological changes induced by RT followed by TPN

(A–C) The liver show inflammatory infiltrates and local necrotic areas (arrows), at varying lobular locations. (A–C) Hematoxylin and eosin; (A) 10x, (B,C) 20x. (D) In places, hepatocyte dropout left loose connective tissue behind that was infiltrated by CD163-positive macrophages and a few lymphoid cells. CD 163, 20x. (E) Reticulin network condensation and fragmentation was evident at the sites of liver necrosis. Reticulin, 10x. (F) Cortical brain (30x) showed enlarged Alzheimer type II astrocytes with chromatin displacement (arrows) consistent with hepatic encephalopathy. Hematoxylin and eosin, 30x.